

H_0 from Type Ia Supernovae

By G. A. TAMMANN¹, A. SANDAGE² AND A. SAHA³

¹Astronomisches Institut der Universität Basel
Venusstrasse 7, CH-4102 Binningen, Switzerland

²The Observatories of the Carnegie Institution of Washington
813 Santa Barbara Street, Pasadena, CA 91101

³National Optical Astronomy Observatories
950 North Cherry Ave., Tucson, AZ 85726

The Hubble diagrams in B , V , and I of a complete sample of 35 SNe Ia with $(B - V) < 0.06$ and $1200 < v \lesssim 30\,000 \text{ km s}^{-1}$ have a scatter of only 0^m1 , after small corrections are applied for differences in decline rate Δm_{15} and color $(B - V)$. The tightness of the Hubble diagrams proves blue SNe Ia to be the best “standard candles” known. Their absolute magnitudes $M_{B,V,I}$ are calibrated by eight SNe Ia with Cepheid distances from *HST*. Combining this calibration with the appropriate Hubble diagrams yields a large-scale value of $H_0 = 58.5 \pm 6.3$ at the 90-percent confidence level.

The Hubble diagram of SNe Ia has so small scatter that it seems feasible to determine Λ “locally”, i.e. within $z \lesssim 0.12$, once 100-200 SNe Ia with good photometry will be available. Such a local determination would minimize evolutionary effects and K-term corrections.

Clusters of galaxies have provided useful Hubble diagrams through brightest cluster members, TF distances, and $D_n - \sigma$ and fundamental plane distances, but with significantly more scatter ($\sigma = 0^m2 - 0^m3$) than SNe Ia. The zeropoint calibration of these Hubble diagrams is an additional problem, which is aggravated by the high weight of any adopted distance of the Virgo cluster and by selection effects of clusters with only few well studied members. If a Virgo cluster modulus of $(m - M) = 31.60 \pm 0.20$ is adopted for calibration, — a value which is well secured by Cepheids, SNe Ia, and the TF method, and which also agrees with less definitive distances from the globular cluster luminosity function, novae, and the $D_n - \sigma$ method, — one finds $H_0 = 55 \pm 5$. The reasons are explained why some authors have found higher values from clusters.

The determination of H_0 from field galaxies is beset by selection effects of magnitude-limited samples (Malmquist bias). Authors who have properly allowed for bias have consistently obtained $H_0 \approx 55 \pm 5$ within $v \lesssim 5000 \text{ km s}^{-1}$ based on the TF and other methods. The calibration rests only on Cepheids, independent of any adopted Virgo cluster modulus.

Giving highest weight to SNe Ia it is concluded that $H_0 = 58 \pm 6$.

1. Introduction

HST has brought an enormous progress in determining extragalactic distances by providing 26 Cepheid distances to late-type galaxies. This is of paramount importance not only for the determination of the Hubble constant H_0 , but increasingly also for the physical understanding of individual galaxies whose linear sizes, luminosities, masses, radiation densities etc. depend on distance. Unfortunately the progress is confined to late-type galaxies, the distances of early-type galaxies having profited only indirectly.

An overview of the Cepheid distances from *HST* is given in Table 1. Cepheids carry by far the largest weight for the foundation of the extragalactic distance scale. Their zeropoint is based on an adopted LMC modulus of 18.50, which is confirmed by various distance indicators to within $\pm 0^m10$. Cepheid distances are uncontroversial to a large extent with possibly remaining small metallicity effects discussed in Section 2.5.

The 26 galaxies with Cepheid distances from *HST*, all beyond the Local Group, yield a

TABLE 1. Cepheid distances from *HST*.

No. of Galaxies	Authors	No. of SNe Ia
18 Cepheid distances	Freedman 2000	1
1 Cepheid distance	Tanvir et al. 1995	1
7 Cepheid distances	Saha et al. 1999, 2000a	8

mean value of $H_0 = 65 \pm 4$ [$\text{km s}^{-1} \text{Mpc}^{-1}$]. Yet these galaxies lie within $v = 1200 \text{ km s}^{-1}$ which is too local for this determination having any cosmic significance.

An additional distance indicator is therefore needed which can be calibrated by means of the available Cepheids and which carries the distance scale out to $\gtrsim 10\,000 \text{ km s}^{-1}$, i.e. well beyond the influence of peculiar and streaming motions. This distance indicator must be *proven* to be reliable and its intrinsic dispersion must be known in order to control selection effects (cf. Section 4).

Many distance indicators have been proposed, but the proof of their reliability is extremely difficult. The demonstration that they can reproduce a limited number of Cepheid distances, which carry themselves individual errors of up to $\sim 0^m2$, is not good enough, and the internal dispersion remains ill defined. Just because various distance indicators are said to agree amongst themselves is no proof that they form a correct distance scale. If they have similar intrinsic dispersion and if each is not corrected for systematic effects of observational bias errors, their agreement is spurious.

The only satisfactory way to prove potential distance indicators to be useful for the determination of H_0 is the demonstration that they define a linear relation of slope 0.2 (corresponding to linear expansion) in the Hubble diagram out to $\gtrsim 10\,000 \text{ km s}^{-1}$. The scatter about this line provides in addition the intrinsic dispersion of the method if proper allowance is made for observational errors and for the influence of peculiar motions which, however, at $10\,000 \text{ km s}^{-1}$, are negligible for all practical purposes.

This requirement of reliable long-range distance indicators is very well met by supernovae of type Ia (SNe Ia), and they can be calibrated by Cepheids. SNe Ia offer therefore the optimum route to H_0 and are discussed in Section 2. Cluster distances follow in Section 3; they also define a useful Hubble diagram, but their zeropoint calibration is still under debate. The most difficult and least satisfactory way to H_0 by means of distances of field galaxies is discussed in Section 4. The conclusions are given in Section 5.

2. H_0 from SNe Ia

This Section is the result of an *HST* project for the luminosity calibration of SNe Ia that also includes L. Labhardt, F.D. Macchetto, and N. Panagia. The collaboration of J. Christensen, B.R. Parodi, H. Schwengeler, and F. Thim at different stages of the project is acknowledged. We thank also the many collaborators who work behind the scene at the Space Telescope Science Institute for their continued support.

2.1. The sample

From a parent population of 67 SNe Ia with known B and V at maximum, ($B_{\text{max}} - V_{\text{max}}) < 0.20$ (In the following $(B - V)$ for short), and $v^{\text{CMB}} \lesssim 30\,000 \text{ km s}^{-1}$ (to minimize cosmological effects; galaxies with $V_{220} > 3000 \text{ km s}^{-1}$ being corrected for the local 630 km s^{-1} motion with respect to the CMB) a sample of 44 SNe Ia was selected which

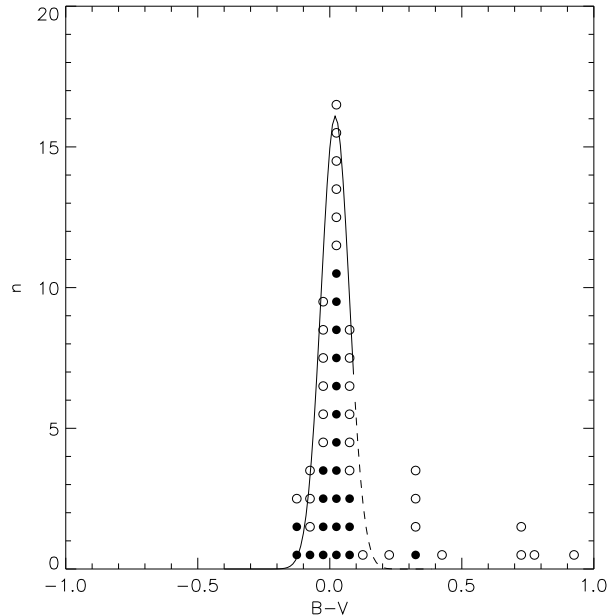


FIGURE 1. The color distribution of all known SNe Ia after 1985 with $v < 30\,000\text{ km s}^{-1}$. Open symbols are for more distant SNe Ia. The binned intervals embrace $\Delta(B - V) = 0^m.05$. A Gaussian fit to all SNe Ia with $(B - V) \leq 0^m.10$ gives $\langle B - V \rangle = 0.020$, $\sigma_{B-V} = 0^m.053$.

fulfill the additional conditions: (1) having occurred after 1985 to ensure photometric quality, and (2) $v_{220} > 1200\text{ km s}^{-1}$ (after correction for Virgocentric infall).

The color cut in $(B - V)$ is justified in Fig. 1 where *all* SNe Ia after 1985 are plotted. Their color distribution is sharply peaked. Some of the 10 red objects with $(B - V) > 0.20$ probably have high internal reddening, others are known to have low expansion velocities (like SN 1986G) or quite peculiar spectra (like SN 1991bg, 1992K). The latter may define special subclasses of SNe Ia and clearly should be excluded from a homogeneous set of SNe Ia. Their exclusion is in any case indicated as long as none of the calibrating SNe Ia is of this type, which is not the case (Section 2.4).

Seven SNe Ia of the blue sample have $0.06 < (B - V) < 0.20$. All seven are underluminous and five of them lie in the inner parts of spiral galaxies. They are therefore suspected to suffer mild absorption in their parent galaxies. Their exclusion is permissible because none of the calibrating SNe Ia is as red.

Two SNe Ia of the blue sample, i.e. SN 1991T (Phillips et al. 1992) and SN 1995ac (Garnavich et al. 1996), had peculiar spectra during their early phases. SN 1991T has long been suspected to be overluminous, but a recent Cepheid distance (Saha et al. 2000a) suggests this overluminosity to be only marginal. SN 1995ac lies, however, significantly above the Hubble line and is certainly overluminous. Both objects are excluded here.

The remaining 35 blue SNe Ia constitute our “fiducial sample”. They are listed in Parodi et al. (2000). Their spectra, as far as available, are Branch-normal. For 29 SNe Ia also $m_I(\text{max})$ is known.

2.2. The color of blue SNe Ia

The mean color of 16 SNe Ia of the fiducial sample, that have occurred in early-type galaxies, is $\langle B - V \rangle = -0.013 \pm 0.015$ and is identical with the mean color of 9 *outlying* SNe Ia in spirals. We therefore take this as the *true* mean intrinsic color of SNe Ia. The

mean intrinsic color derived by Phillips et al. (1999) from different assumptions is bluer by ~ 0.03 . This is irrelevant for the following discussion as long as the calibrating SNe Ia and the remaining objects of the fiducial sample conform with the adopted zeropoint color. (If our adopted mean color was too red, any additional absorption would equally affect the calibrators and the fiducial sample and have no effect on the derived distances). Indeed, after the eight calibrating SNe Ia (Section 2.4) are individually corrected for absorption they exhibit a mean color of $\langle B - V \rangle = -0.009 \pm 0.015$, i.e. only insignificantly different from our adopted mean intrinsic color. Also the 10 remaining SNe Ia of the fiducial sample, which lie in the inner parts of spirals or whose position within their parent spirals is poorly known, are redder by a negligible amount of only $0^m012 \pm 0^m016$.

The scatter in $(V - I)$ is somewhat larger ($\sigma_{V-I} = 0^m08$) than in $(B - V)$, but here again the mean color of $\langle V - I \rangle = -0.276 \pm 0.016$ is the same for the SNe Ia in E/S0 galaxies and in spirals as well as for the calibrating SNe Ia.

2.3. Second-parameter correction

The 35 SNe Ia of the fiducial sample define very tight Hubble diagrams in B , V , and I for the range $1200 < v \lesssim 30\,000 \text{ km s}^{-1}$ (cf. Parodi et al. 2000; their Fig. 3), the scatter being only $\sigma_B = 0^m21$, $\sigma_V = 0^m18$, and $\sigma_I = 0^m16$. This proves their usefulness as “standard candles”.

Although the Hubble diagrams of SNe Ia in B , V , and I are tighter than for any other known objects, they still contain systematic effects. As suspected early on by some authors and pointed out again by Phillips (1993) the peak luminosity of SNe Ia correlates with the decline rate. Phillips introduced Δm_{15} , i.e. the decline in magnitudes during the first 15 days after B maximum, as a measure of the decline rate. Indeed the residuals of the SNe Ia of the fiducial sample correlate with Δm_{15} (Fig. 2a). The relation is roughly $\delta M \propto 0.5 \Delta m_{15}$ in all three colors, slow decliners being brighter.

In addition the luminosities of SNe Ia correlate with the color $(B - V)$ (Tammann 1982; Tripp 1998). The proportionality factor between the magnitude residual δM and $\Delta(B - V)$ decreases from ~ 2.6 in B to ~ 1.2 in I for the fiducial sample, blue SNe Ia being brighter (Fig. 2b). This dependence is significantly shallower than for absorption by standard dust. There are indeed strong reasons (Saha et al. 1999) to believe that the dependence of luminosity on color is an intrinsic effect of SNe Ia.

The “second parameters” Δm_{15} and $(B - V)$ are orthogonal to each other. A simultaneous fit of the residuals δM in function of Δm_{15} and $(B - V)$ is therefore indicated. In that case the fiducial sample yields (Parodi et al. 2000)

$$\delta M_B^{\text{corr}} = 0.44_{\pm 0.13} (\Delta m_{15} - 1.2) + 2.46_{\pm 0.46} [(B - V) + 0.01] - 28.40_{\pm 0.16}, \sigma_B = 0.129 \quad (2.1)$$

$$\delta M_V^{\text{corr}} = 0.47_{\pm 0.11} (\Delta m_{15} - 1.2) + 1.39_{\pm 0.40} [(B - V) + 0.01] - 28.39_{\pm 0.14}, \sigma_V = 0.129 \quad (2.2)$$

$$\delta M_I^{\text{corr}} = 0.40_{\pm 0.13} (\Delta m_{15} - 1.2) + 1.21_{\pm 0.43} [(B - V) + 0.01] - 28.11_{\pm 0.17}, \sigma_I = 0.122 \quad (2.3)$$

It is interesting to note that the residuals δM correlate also with the Hubble type (SNe Ia in early-type galaxies being fainter) and marginally so with the radial distance from the galaxy center, but that these dependencies disappear once the apparent magnitudes are corrected for Δm_{15} and $(B - V)$.

The apparent magnitudes $m_{B,V,I}^{\text{corr}}$ of the 35 SNe Ia, corrected for Δm_{15} and color by means of equations (2.1) - (2.3), define Hubble diagrams as shown in Fig. 3. *Their tightness is astounding.* The Cerro Tololo collaboration, to whom one owes 70 percent of the photometry of the fiducial sample, quote a mean observational error of their m_{max} -values of $\sim 0^m10$ and of their colors $(B - V)$ of $\sim 0^m05$. This alone would suffice to explain the observed scatter of $\sigma_m = 0^m12 - 0^m13$. An additional error source are the corrections for Galactic absorption which were adopted from Schlegel et al. (1998). In fact, if

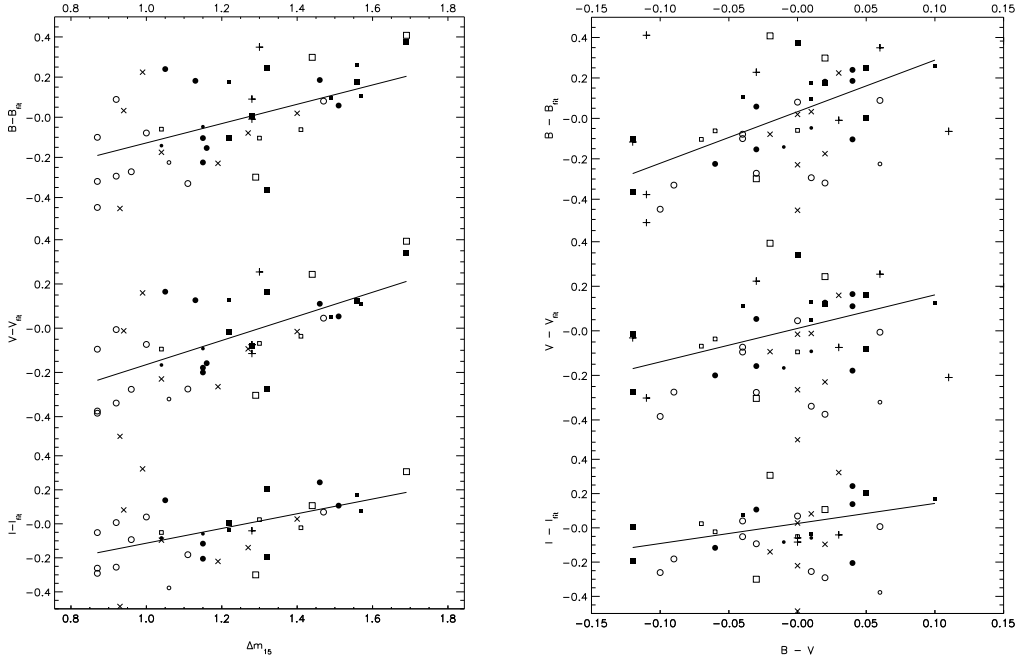


FIGURE 2. *Left panel:* Relative magnitudes (i.e. residuals from the Hubble line) for the SNe Ia of the fiducial sample in function of the decline rate Δm_{15} . Circles are SNe Ia in spirals, squares in E/S0 galaxies. Open symbols are SNe Ia with $1200 < v < 10\,000 \text{ km s}^{-1}$, closed symbols are for more distant SNe Ia. Small symbols are SNe Ia whose observations begin eight days after B maximum or later. Neither the SNe Ia before 1985 with known Δm_{15} (shown as crosses) nor the seven blue, but reddened SNe Ia (shown as X's) are considered for the weighted least-squares solutions (solid lines). *Right panel:* Relative absolute magnitudes (i.e. residuals from the Hubble line) for the SNe Ia of the fiducial sample in function of their color ($B - V$). Symbols as in the left panel.

one excludes the nine SNe Ia with large Galactic absorption corrections ($A_V > 0^m2$) the scatter decreases to 0^m11 in all three colors. Two important conclusions follow from this. (1) If the total observed scatter of the Hubble diagrams is read vertically as an effect of peculiar motions, a generous upper limit is set of $\Delta v/v = 0.05$, which holds for the range of $3500 \lesssim v \lesssim 30\,000 \text{ km s}^{-1}$. The (all-sky) distance-dependent variation of H_0 must be even smaller. (2) If on the other hand the scatter is read horizontally and if allowance is made for the observational errors of the apparent magnitudes (and for any peculiar motions) one must conclude that the luminosity scatter of blue SNe Ia, once they are homogenized in Δm_{15} and color, is smaller than can be measured at present. With other words, they are extremely powerful standard candles.

It is obvious that if one can determine the absolute magnitude of a few (nearby) SNe Ia this offers what we believe to be a definitive route to determine the large-scale value of H_0 .

2.4. The luminosity calibration of SNe Ia

As stated before, *HST* has provided Cepheid distances to nine galaxies which have produced 10 SNe Ia. Excluding the spectroscopically peculiar SN 1991T in NGC 4527 (Saha et al. 2000a) leaves eight galaxies with nine SNe Ia. They are listed in Table 2.

The weights of the individual values of M in Table 2 are quite different due to the different quality of the SNe Ia light curves and of the Cepheid distances, but they are

TABLE 2. Absolute B , V , and I magnitudes of blue SNe Ia calibrated through Cepheid distances of their parent galaxies.

SN (1)	Galaxy (2)	$(m-M)^0$ (3)	ref. (4)	M_B^0 (5)	M_V^0 (6)	M_I^0 (7)	Δm_{15} (8)
1895 B	NGC 5253	28.01 (08)	2	-19.54 (22)
1937 C	IC 4182	28.36 (09)	1	-19.56 (15)	-19.54 (17)	...	0.87 (10)
1960 F	NGC 4496A	31.04 (10)	3	-19.56 (18)	-19.62 (22)	...	1.06 (12)
1972 E	NGC 5253	28.61 (08)	2	-19.64 (16)	-19.61 (17)	-19.27 (20)	0.87 (10)
1974 G	NGC 4414	31.46 (17)	4	-19.67 (34)	-19.69 (27)	...	1.11 (06)
1981 B	NGC 4536	31.10 (05)	5	-19.50 (14)	-19.50 (10)	...	1.10 (07)
1989 B	NGC 3627	30.22 (12)	6	-19.47 (18)	-19.42 (16)	-19.21 (14)	1.31 (07)
1990 N	NGC 4639	32.03 (22)	7	-19.39 (26)	-19.41 (24)	-19.14 (23)	1.05 (05)
1998 bu	NGC 3368	30.37 (16)	8	-19.76 (31)	-19.69 (26)	-19.43 (21)	1.08 (05)
mean (straight, excl. SN 1895 B)				-19.57 (04)	-19.56 (04)	-19.26 (06)	1.06 (05)
mean (weighted, excl. SN 1895 B)				-19.55 (07)	-19.53 (06)	-19.25 (09)	1.08 (02)
$M^{\text{corr}}(\Delta m_{15} = 1.2; (B - V) = -0.01)$				-19.48 (07)	-19.47 (06)	-19.19 (09)	1.08 (02)

References — (1) Saha et al. 1994 (2) Saha et al. 1995 (3) Saha et al. 1996b (4) Turner et al. 1998 (5) Saha et al. 1996a (6) Saha et al. 1999 (7) Saha et al. 1997 (8) Tanvir et al. 1995.

also relatively strongly affected by the corrections for internal absorption. The estimated individual errors are compounded and carried on to determine the total weights. This procedure is much safer than to exclude single SNe Ia for the one or the other reason.

The adopted mean absolute magnitudes in Table 2 agree fortuitously well with explosion models, ejecting about $0.6 M_{\odot}$ of ^{56}Ni , by Höflich & Khokhlov (1996) for equally blue SNe Ia (cf. also Branch 1998).

The *HST* photometry for the Cepheids in the galaxies listed in Table 2 (except NGC 4414) has been re-analyzed by Gibson et al. (2000). For 114 Cepheids in common with Saha et al. (1994, 1995, 1996a,b, 1997, 1999) they find a brighter photometric zeropoint by $0^{\text{m}}04 \pm 0^{\text{m}}02$, which is as satisfactory as can be expected from the subtle photometry with WFPC-2. On the other hand a recent check on the zeropoint by A. Saha suggests that it should become fainter by $0^{\text{m}}02$.

Gibson et al. (2000) have added Cepheids which were reduced only with the photometric ALLFRAME package. Many of the additional Cepheids had also been detected by us, but were discarded because of what we considered to be insuperable problems such as poor light curves or excess crowding. With their additional Cepheids Gibson et al. (2000) have derived a distance modulus of NGC 5253 that is $0^{\text{m}}39$ smaller than listed in Table 2. Their reduction is unlikely for us because it would imply a very faint tip of the red-giant branch. For the remaining galaxies in Table 2 they suggest a mean decrease of the distance moduli by $0^{\text{m}}11 \pm 0^{\text{m}}03$. This would lead to an increase of H_0 by 5-6 percent. We do not consider this possibility pending independent confirmation of the ALLFRAME Cepheids.

2.5. The value of H_0

Combining the weighted mean absolute magnitude M_{BVI}^0 of SNe Ia from Table 2 with the observed Hubble diagrams in B , V , and I of the fiducial sample, corrected only for Galactic absorption, leads immediately to a mean value of $H_0(BVI) = 58.3 \pm 2.0$ (internal error) (cf. Parodi et al. 2000). The three colors B , V , and I give closely the same results.

However, the calibrating SNe Ia lie necessarily in late-type galaxies (because the parent galaxies must contain Cepheids), and these SNe Ia are therefore expected to be somewhat

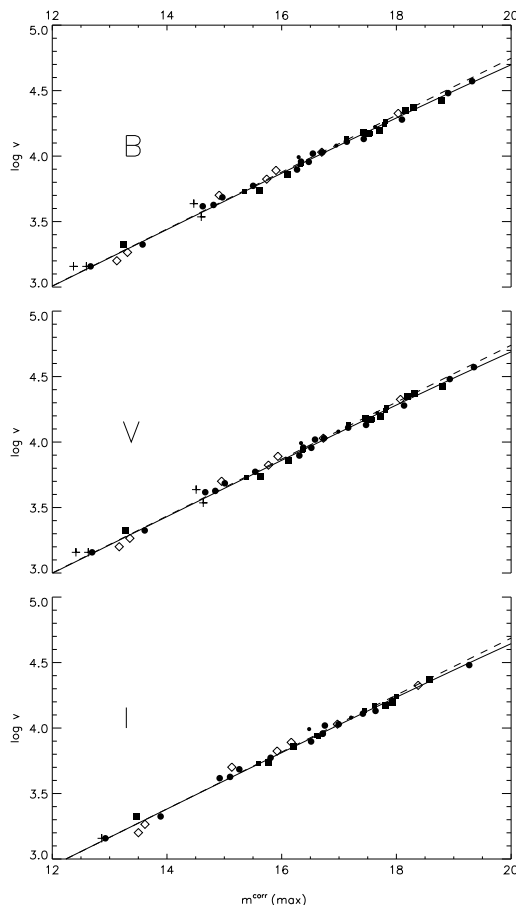


FIGURE 3. The Hubble diagrams in B , V , (and I) for the 35 (29) SNe Ia of the fiducial sample with magnitudes m^{corr} , i.e. corrected for decline rate Δm_{15} and color ($B - V$) (equations 2.1 - 2.3). Circles are SNe Ia in spirals, squares in E/S0 galaxies. Small symbols are SNe Ia whose observations begin eight days after B maximum or later. Solid lines are fits to the data assuming a flat universe with $\Omega_M = 0.3$ and $\Omega_\Lambda = 0.7$; dashed lines are linear fits with a forced slope of 0.2 (corresponding approximately to $\Omega_M = 1.0$ and $\Omega_\Lambda = 0.0$). Not considered for the fits are the SNe Ia before 1985 and the seven SNe Ia with $0.06 < (B - V) < 0.20$ that are suspected to be reddened. They are shown as diamonds after absorption correction; their inclusion would have nil effect on the fit.

more luminous than their counterparts of the fiducial sample which lie in galaxies of all Hubble types (cf. Section 2.3). Because of the correlation between Hubble type and decline rate Δm_{15} , the calibrators should have also slower decline rates than average. This is indeed the case. Consequently the calibrators and the fiducial sample should be homogenized as to Δm_{15} , i.e. the corrected magnitudes M_{BVI}^{corr} from Table 2 should be compared with the corrected Hubble diagram in Fig. 3. It may be noted that the correction for variations in color ($B - V$) has here no net effect because the calibrators and the fiducial sample have identical mean colors.

An exact comparison should allow for the fact that cosmological effects on the Hubble diagram are non-negligible at $\sim 30\,000 \text{ km s}^{-1}$. Three different model universes are therefore fitted to the data as illustrated in a differential Hubble diagram (Fig. 4):

1. A flat Universe with $\Omega_M = 1.0$ ($q_0 = 0.5$; Sandage 1961, 1962). When the magnitudes

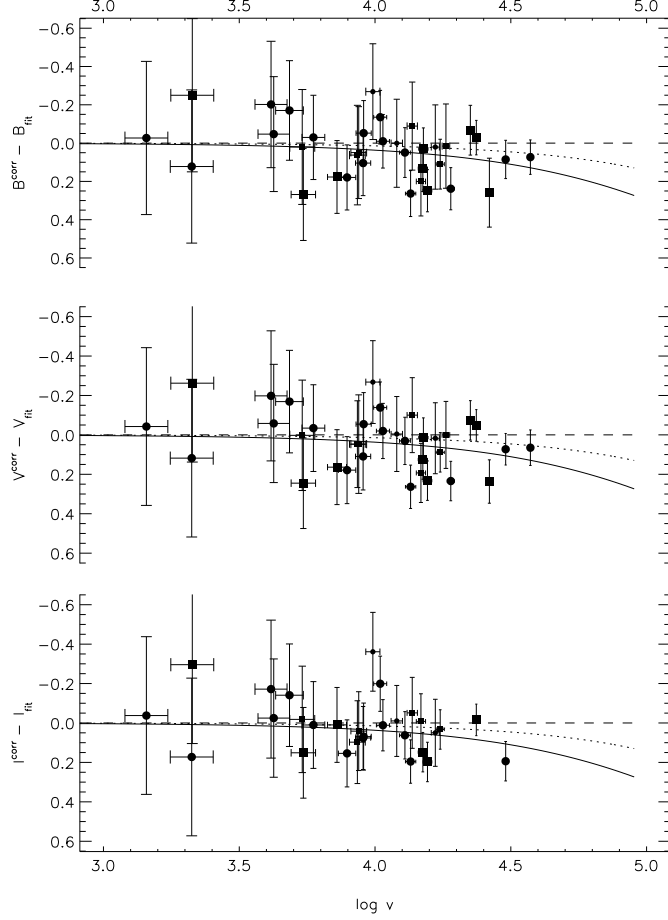


FIGURE 4. Differential Hubble diagrams ($m^{\text{corr}} - m_{\text{fit}}$) vs $\log v$ in B , V , (and I) for the 35 (29) SNe Ia of the fiducial sample. Symbols as in Fig. 3. The dashed line is for a flat cosmological model with $\Omega_M = 1.0$ and $\Omega_\Lambda = 0.0$; the theoretical apparent magnitudes m_{fit} correspond to this model. The full line is for a flat model with $\Omega_M = 0.3$ and $\Omega_\Lambda = 0.7$; the dotted line is for an open universe with $\Omega_M = 0.2$ and $\Omega_\Lambda = 0.0$.

m_{BVI}^{corr} of the fiducial sample are fitted to the corresponding Hubble line one obtains, after inserting $\langle M_{BVI}^{\text{corr}} \rangle$ of the calibrators, $H_0(B) = 60.2 \pm 2.1$. The values in V and I are very similar (60.1 and 60.0, respectively).

2. An open Universe with $\Omega_M = 0.2$ ($q_0 = 0.1$; Sandage 1961, 1962). The fit is in this case somewhat better, giving $H_0(BVI) = 60.2 \pm 2.0$.

3. A flat Universe with $\Omega_M = 0.3$, $\Omega_\Lambda = 0.7$ ($q_0 = -0.55$). This model is favored by *high-redshift* SNe Ia (Perlmutter 1998, Riess et al. 1998, Schmidt et al. 1998, Perlmutter et al. 1999). The Hubble line is given in this case by (cf. Carroll, Press, & Turner 1992)

$$m_{B,V,I} = 5 \log \left(\frac{c}{H_0} (1+z_1) \int_0^{z_1} [(1+z)^2 (1 + \Omega_M z) - z(2+z)\Omega_\Lambda]^{-1/2} dz \right) + M_{B,V,I} + 25. \quad (2.4)$$

This model gives the best fit to the fiducial sample and yields, after insertion of $\langle M_{BVI}^{\text{corr}} \rangle$ from Table 2, $H_0(B) = 61.0 \pm 2.1$, $H_0(V) = 60.9 \pm 1.8$, and $H_0(I) = 60.7 \pm 2.6$. A mean value of $H_0 = 60.9 \pm 1.8$ is adopted for the following discussion.

The three model Universes can be distinguished with the present fiducial sample only at the 1σ -level. But the possibility to determine Λ from rather local SNe Ia is interesting in principle. The advantage would be good multi-color photometry (e.g. in B, V, I), allowing homogenization of the SNe Ia in color and good control of internal absorption, quite small K-corrections, and short look-back times minimizing evolutionary effects. From 100-200 SNe Ia with good observations and $z < 0.12$ one should obtain a significant value of Λ .

2.6. Discussion

It should be noted that the second-parameter corrections increase H_0 by only 4.3 percent, i.e. from 58.3 to 60.9. This is supported by the fact that if one restricts the discussion to SNe Ia in spirals, minimizing in this way the difference between the parent galaxies of the calibrators and of the SNe Ia of the fiducial sample, one obtains $H_0(BVI) = 59.1$ independent of any second-parameter correction. Alternatively, if one considers the 21 SNe Ia of the fiducial sample with $\Delta m_{15} \geq 1.3$, whose mean decline rate of $\langle \Delta m_{15} \rangle = 1.08 \pm 0.02$ is the same as that of the calibrators, one obtains $H_0(BVI) = 59.2$ (Parodi et al. 2000).

Other authors have derived from part of the fiducial sample and from all or some of the calibrators in Table 2 values from $H_0 = 50 \pm 3$ (Lanoix 1998) to $H_0 = 72 \pm 4$ (Richtler & Drenkhahn 1999). Intermediate values of $H_0 = 63 - 64 \pm 2.2$ were found by Suntzeff et al. (1999) and Phillips et al. (1999), however they base their result on a significantly steeper Δm_{15} -luminosity correction than found here. This would lead to an overcorrection of the larger fiducial sample used here. If their correction was applied to the present data, one would obtain $H_0 = 59.7$ for the SNe Ia with $\Delta m_{15} < 1.2$ ($n=17$), and $H_0 = 64.6$ for those with $\Delta m_{15} \geq 1.2$ ($n=18$). Since seven of the eight calibrators fall into the first category, the lower value must be more nearly correct.

By relying exclusively on the Cepheid distances by Gibson et al. (2000; cf. Section 2.4), Freedman (2000) was able to push the solution of Suntzeff et al. (1999) and Phillips et al. (1999) up to $H_0 = 68$.

Riess et al. (1998) employed a so-called ‘‘Multi Light Curve Shape’’ (MLCS) method to correct simultaneously for Galactic absorption and the relative SN Ia luminosity. The resulting distance moduli (their Table 10) imply, however, that H_0 depends on their correction parameter Δ , i.e. $\langle H_0 \rangle = 66.6 \pm 1.1$ for $\Delta < -0.20$ ($n=9$) and $\langle H_0 \rangle = 61.8 \pm 1.3$ for $\Delta > -0.20$ ($n=18$). Jha et al. (1999) employed also the MLCS method to derive $H_0 = 64 \pm 7$ without listing Δ -values of individual SNe Ia. Tripp & Branch (1999), correcting for Δm_{15} and color ($B - V$), have obtained $H_0 = 62 (\pm 4)$.

The present result of $H_0 = 60.2 \pm 2.1$ is still affected by external errors. Yet the largest systematic error source of all distance indicators that depend on an adopted mean luminosity (or size), i.e. selection effects against underluminous (or undersized) ‘‘twins’’, is negligible in the case of blue SNe Ia because of their exceptionally small luminosity dispersion.

External errors of either sign are introduced (cf. Parodi et al. 2000) by the photometric zeropoint of the WFPC-2 photometry (0^m04), by the adopted slope of the Δm_{15} -luminosity relation (0^m02), by the velocity correction for Virgocentric infall and by the correction for motion relative to the CMB (0^m02).

Other errors are asymmetric with a tendency to underestimate distances. The adopted LMC modulus of 18.50 for the zeropoint of the Cepheid PL relation is probably too small by $\sim 0^m06$ (eg. Federspiel, Tammann, & Sandage 1998; Madore & Freedman 1998; Feast 1999; Walker 1999; Gilmozzi & Panagia 1999; Gratton 2000; Sakai, Zwitsky, & Kennicutt 2000). Smaller LMC moduli suggested on the basis of statistical parallaxes of

RR Lyrae stars and red giant clump stars depend entirely on the sample selection and on the absence of metallicity and evolutionary effects, respectively. The higher LMC modulus will increase all moduli by $0^m06 \pm 0^m10$. Incomplete Cepheid sampling near the photometric threshold always tends to yield too short distances (Sandage 1988a; Lanoix, Paturel, & Garnier 1999; Mazumdar & Narasimha 2000). The effect is estimated here to be $0^m05 \pm 0^m05$. Stanek & Udalski (1999) have proposed that photometric blends of Cepheids in very crowded fields lead to a serious underestimate of the distances. Careful analyses by Saha et al. (2000b) and Ferrarese et al. (2000) show the effect to be more modest for the Cepheid distances in Table 2, say $0^m03 \pm 0^m03$ on average. Absorption corrections of the calibrating SNe Ia and those of the fiducial sample, having identical colors after correction, enter only differentially. However, if one excludes the nine SNe Ia with large Galactic absorption (Section 2.3) the Hubble line of Fig. 3 shifts faintwards by 0^m05 in B . Finally seven SNe Ia were excluded on the suspicion of having some internal absorption (Section 2.1). If they had been included after being corrected for absorption, their effect on the Hubble line would be negligible. If, however, their colors are intrinsic they would shift the Hubble line by 0^m02 towards fainter magnitudes. Combining the absorption errors it is estimated that the distances of the fiducial sample are too small by $0^m05 \pm 0^m05$ on average. Finally there is much discussion of the metallicity effect on Cepheid distances. Theoretical investigations show this effect to be nearly negligible (Sandage, Bell, & Tripicco 1999; Alibert et al. 1999) Other authors do not even agree on the sign of the correction. Based on Kennicutt et al. (1998) Gibson et al. (2000) have concluded that the Cepheid distances in Table 4 are too small by 0^m07 due to variations of the metallicity. A distance increase of $0^m04 \pm 0^m10$ is adopted as a compromise.

Adding the various error sources in quadrature leads to a correction factor of 0.96 ± 0.08 which is to be applied to $H_0 = 60.2 \pm 2.1$. At a 90-percent confidence level one obtains then

$$H_0 = 58.5 \pm 6.3. \quad (2.5)$$

If only the Cepheid distances of Gibson et al. (2000; cf. Section 2.4) had been used, excluding their unlikely value for NGC 5253, one would have obtained $H_0 = 61.6 \pm 6.6$.

The standards for the determination of H_0 are now set by SNe Ia. In the next Section it will be asked to what extent these standards can be met by other distance indicators, i.e. how reliable are they as relative distance indicators and how accurate is their zeropoint calibration?

3. H_0 from Cluster Distances

3.1. The Hubble diagram of clusters

3.1.1. Brightest cluster members

A deep (to $z = 0.45$) and tight ($\sigma_m = 0^m32$) Hubble Diagram is that of 1st-ranked E and S0 cluster galaxies corrected for Galactic absorption, aperture effect, K-dimming, Bautz-Morgan effect, and cluster richness (Sandage & Hardy 1973). They define a Hubble line in the range of $1200 < v < 30\,000 \text{ km s}^{-1}$ of

$$\log v = 0.2 m_{V_c} + (1.359 \pm 0.018); \quad \sigma_{m_V} = 0.32; \quad n = 76 \quad (3.6)$$

which is easily transformed into

$$\log H_0 = 0.2 M_V(1st) + (6.359 \pm 0.018). \quad (3.7)$$

Weedman (1976) has established a Hubble diagram using the mean magnitude of the 10 brightest cluster members. The small scatter of $\sigma_{m_{10}} = 0^m15$ is not directly comparable

with other values because the magnitudes are defined within a *metric* diameter and depend somewhat on redshift.

Another Hubble diagram of 1st-ranked galaxies has been presented by Lauer & Postman (1992). It comprises the complete sample of 114 Abell clusters with $v < 15\,000\text{ km s}^{-1}$. The scatter about the mean Hubble line amounts to $\sigma_m = 0^m3$.

3.1.2. The Tully-Fisher (TF) relation

Dale et al. (1999) have derived *relative I-band TF distances* of 52 clusters from an average of 8-9 members per cluster. The *mean* cluster distances define a Hubble line with a scatter of only $\sigma_{(m-M)} = 0^m12$, i.e. similar to SNe Ia. The clusters are corrected for *differential* selection bias, but the data are still unsuitable to derive absolute distances because with only a few members per cluster the Teerikorpi cluster incompleteness bias must be severe (Section 3.4). The same holds for an older sample of 18 clusters by Giovanelli et al. (1997), for which Sakai et al. (2000) have derived *I-band TF distances*. Sixteen of their clusters with $1500 < v < 9000\text{ km s}^{-1}$ and each with 15 studied galaxies on average define a Hubble line with a scatter of $\sigma_{(m-M)} = 0^m18$, which implies a scatter of $\sigma > 0^m5$ of the TF modulus of an individual galaxy.

3.1.3. The $D_n - \sigma$ relation

Kelson et al. (2000) have derived $D_n - \sigma$ and fundamental plane (FP) distances of (only) 11 clusters out to $v \sim 10\,000\text{ km s}^{-1}$. The two resulting sets define Hubble diagrams with a remarkably small scatter of $\sigma_{(m-M)} = 0^m19$.

3.1.4. Combining different Hubble diagrams

A combination of data of brightest cluster galaxies and $D_n - \sigma$ measurements by Faber et al. (1989) have been used to derive cluster distances relative to the Virgo cluster (Jerjen & Tammann 1993). When these are augmented by the relative TF distances of clusters by Giovanelli (1997) one obtains a Hubble diagram as shown in Fig. 5. The data scatter by $\sigma_{(m-M)} = 0^m20$ about a Hubble line. The latter is found by linear regression and implies

$$\log H_0 = -0.2(m - M)_{\text{Virgo}} + (8.070 \pm 0.007). \quad (3.8)$$

(Federspiel, Tammann, & Sandage 1998). The equation is particularly useful because the calibration of H_0 can simply be accomplished by inserting the Virgo cluster modulus.

It should be noted that the observed scatter of the above Hubble diagrams is almost entirely due to intrinsic scatter of the distance indicators and to measurement errors because the contribution of peculiar velocities is $\lesssim 0^m1$ as shown by the Hubble diagram of SNe Ia (Fig. 3).

3.2. Relative distances of local groups and clusters

The reliability of other distance indicators, which have failed so far to establish a Hubble diagram, can be tested by comparing their relative distances of local groups or clusters, specifically between the Leo I group, the Virgo cluster, and the Fornax cluster. It is a most gentle test because the mean distances from several member galaxies are compared and the problem of the zeropoint calibration does not enter.

In Table 3 the modulus differences Virgo-Leo I, Fornax-Virgo, and Fornax-Leo I are listed as derived from various distance indicators. The sources of these differences are also listed. The first four lines show the differences of the distance indicators which have passed the Hubble diagram test. The fifth line gives the relative moduli as derived from the mean group/cluster velocities. Most of the entries are in statistical agreement with the weighted means in the sixth line.

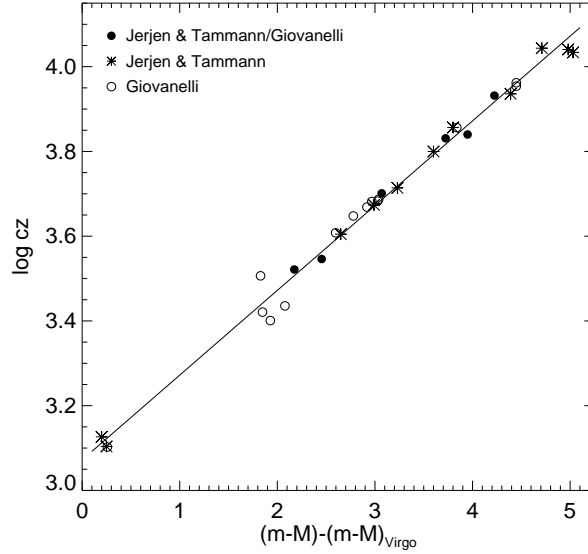


FIGURE 5. Hubble diagram of 31 clusters with known relative distances. Asterisks are data from Jerjen & Tammann (1993). Open circles are from Giovanelli (1997). Filled circles are the average of data from both sources.

There are, however, four entries shown in parentheses, which deviate significantly from the adopted means. The result of the FP that the Fornax cluster is more distant by as much as 0^m5 than the Virgo cluster is very unlikely. The TF distance of the Leo I group carries little weight being based on only three galaxies, and the small TF distance of the Fornax cluster, i.e. 0^m40 nearer than the Virgo cluster, is simply impossible. A compilation (Tammann & Federspiel 1997) of the relative distance Fornax-Virgo, as determined by 30 different authors, suggests Fornax to be slightly more distant than Virgo in agreement with the adopted means in Table 3, but all attempts to determine the TF distance of Fornax have come out with suspiciously small values. The discrepancy is not sufficiently explained by the fact that even a complete sample of the Fornax cluster contains only eight full-size spirals suited for the TF method in addition to 19 small late-type galaxies with large scatter. The discrepancy remains hence enigmatic. The case shows the possibility that even tested distance indicators may fail in individual cases.

In the lower part of Table 3 the relative distances are shown by different authors from planetary nebulae (PNe), the surface brightness fluctuations (SBF) and of the globular cluster luminosity function (GCLF). The modulus differences of the PNe are rather small. In particular the value of Virgo-Leo I is $0^m39 \pm 0^m17$ smaller than adopted. This unsatisfactory result of the PNe does not come as a surprise. The method rests on the assumption that the luminosity of the brightest planetary shell, as seen in a bright emission line, is a fixed standard candle and does not depend on sample size (i.e. galaxy luminosity). This is not only against the expectation from any realistic luminosity function, but is also contradicted by observations (Bottinelli et al. 1991; Tammann 1993; Soffner et al. 1996). Moreover the shell luminosity is predicted to depend on metallicity and age (Méndez et al. 1993).

Also the SBFs give a small difference Virgo-Leo I and an almost certainly too large difference Fornax-Virgo. If the quoted small errors are taken at face value the method

TABLE 3. Relative distances of Leo I, Virgo, and Fornax from various distance indicators. (The errors shown are from the quoted sources)

Method (1)	$\Delta(m - M)$ Virgo–Leo I (2)	$\Delta(m - M)$ Fornax–Virgo (3)	$\Delta(m - M)$ Fornax–Leo I (4)	Source (5)
Cepheids, SNe Ia	1.37 ± 0.21	0.05 ± 0.22	1.42 ± 0.10	Tables 4 and 6
$D_n - \sigma$	0.92 ± 0.32	0.17 ± 0.16	1.09 ± 0.32	Faber et al. 1989
FP	...	(0.52 ± 0.17)	...	Kelson et al. 2000
TF ($BVRI$)	$(1.95 \pm 0.23)^1$	(-0.40 ± 0.10)	$(1.55)^1$	Schröder 1995
vel. ratio ²	1.29 ± 0.31	0.27 ± 0.30	1.57 ± 0.18	Kraan-Korteweg 1986
mean:	1.25 ± 0.15	0.15 ± 0.12	1.43 ± 0.08	
PNe	0.86 ± 0.09	0.33 ± 0.09	1.19 ± 0.10	Ferrarese et al. 2000
SBF	0.88 ± 0.07	0.40 ± 0.05	1.28 ± 0.06	Ferrarese et al. 2000
	0.93 ± 0.05	0.37 ± 0.04	1.30 ± 0.05	Tonry et al. 2000
GCLF	1.62 ± 0.31	-0.35 ± 0.14	1.27 ± 0.31	Tammann & Sandage 1999
	1.69 ± 0.56	0.14 ± 0.07	1.83 ± 0.56	Ferrarese et al. 2000

¹ From only 3 spirals in the Leo I group (Federspiel 1999)

² Assuming $v_{220}(\text{Leo}) = 648$, $v_{220}(\text{Virgo}) = 1179$, $v_{220}(\text{Fornax}) = 1338 \text{ km s}^{-1}$ (Kraan-Korteweg 1986) and allowing for a peculiar velocity of Leo I of 100 km s^{-1} and of Fornax of 200 km s^{-1}

is incompatible with the adopted relative position Leo I–Virgo–Fornax. In any case the method should be given low weight until its real capabilities are proved beyond doubt.

The distance differences of the GCLFs listed in Table 3 have too large errors and differ too much between different authors, due to different sample selections, that any clear conclusion could be drawn. In the case of the Virgo cluster it yields a perfect distance determination (cf. Table 5); in other cases it gives quite erratic results (Tammann & Sandage 1999).

3.3. The distance of the Virgo cluster and of other clusters

Four galaxies with known Cepheid distances lie in the Virgo cluster proper, i.e. within the isopleths and the X-ray contours (cf. Binggeli, Popescu, & Tammann 1993). As can be seen in Table 4 they have widely different distances. Three of the galaxies have been selected from the atlas of Sandage & Bedke (1988) on grounds of their exceptionally good resolution; they are therefore *expected* to lie on the near side of the cluster. The fourth galaxy, NGC 4639, which has a *low* recession velocity and can therefore not be assigned to the background, but must be a dynamical member of the cluster, is more distant by almost 1^m0 and must lie on the far side of the extended cluster. The relative position of the four galaxies is fully confirmed by their TF distances. The cluster *center* must lie somewhere between the available Cepheid distances, say at $(m - M) = 31.5 \pm 0.3$. Much of the confusion of the extragalactic distance scale comes from the ill-conceived notion that the three highly resolved Virgo galaxies could reflect the *mean* distance of the cluster.

Three well observed SNe Ia have appeared in Virgo cluster members. Their distances in Table 4, corrected for decline rate Δm_{15} and color ($B - V$), have been calculated from their individual parameters as compiled by Parodi et al. (2000) and from the calibration in Table 2.

The best possible application of the TF method is provided by the Virgo cluster,

TABLE 4. Distances of the Virgo and Fornax clusters

Virgo				Fornax			
Object (1)	$(m - M)^0$ (2)	Ref. (3)	Remarks (4)	Object (5)	$(m - M)^0$ (6)	Ref. (7)	Remarks (8)
Cepheids							
NGC 4321	31.04	1	highly resolved	NGC 1326A	31.49	7	
NGC 4535	31.10	2	highly resolved	NGC 1365	31.39	8	
NGC 4548	31.04	3	highly resolved	NGC 1425	31.81	9	
...							
NGC 4639	32.03 (!)	4	normal resolved				
mean:	~ 31.5				31.56 ± 0.13		
SNe Ia							
SN 1984A	31.42	5	in NGC 4419	SN 1980N	31.76	5	in NGC 1316
SN 1990N	32.12	5	in NGC 4639	SN 1981D	31.51	5	in NGC 1316
SN 1994D	31.27	5	in NGC 4526	SN 1992A	31.84	5	in NGC 1380
mean:	31.60 ± 0.30				31.70 ± 0.10		
Tully-Fisher Relation (complete samples)							
mean (n=49):	31.65 ± 0.25	6			(31.25 ± 0.10)	10	
overall mean:	31.60 ± 0.20			overall mean:	31.65 ± 0.08		

References — (1) Ferrarese et al. 1996 (2) Macri et al. 1999 (3) Graham et al. 1999 (4) Saha et al. 1997 (5) see text (6) Federspiel et al. 1998; Federspiel 1999 (7) Prosser et al. 1999 (8) Silbermann et al. 1999 (9) Mould et al. 2000 (10) Schröder 1995; Federspiel 1999

because a very deep catalog of the cluster (Binggeli, Sandage, & Tammann 1985) allows selection of a *complete* sample of all 49 sufficiently inclined cluster spirals. They define a reliable position and slope of the TF relation in B (Fig. 6b). (It is sometimes argued that I -magnitudes [albeit incomplete!] should be used to minimize the internal-absorption correction, but the advantage is offset by the steeper slope of the TF relation at long wavelengths [Schröder 1995]). Combining these data with the excellent calibration of the TF relation (Fig. 6a), which rests now on 26 galaxies with Cepheid distances and 2 companions of M 101, for which a Cepheid distance is available, yields the TF modulus shown in Table 4.

The distance of the Virgo cluster is such an important milestone for the extragalactic distance scale that the value adopted in Table 4 should be compared with other distance indicators. Three distance indicators of early-type galaxies shall be considered, although their reliability is much less tested. (1) The peak of the luminosity function of globular clusters (LFGC) is interesting because its calibration of the zeropoint rests on the Cepheid distance of M 31 *and* in excellent agreement on the RR Lyrae distance of Galactic globular clusters. (2) Six known novae in Virgo cluster ellipticals can be compared to the novae in M 31 whose *apparent* distance modulus can be derived from Cepheids *or* from Galactic novae (Capaccioli et al. 1989). Alternatively the semi-theoretical zeropoint of novae can be taken from Livio (1997). (3) The $D_n - \sigma$ relation can be applied to E/S0 galaxies and

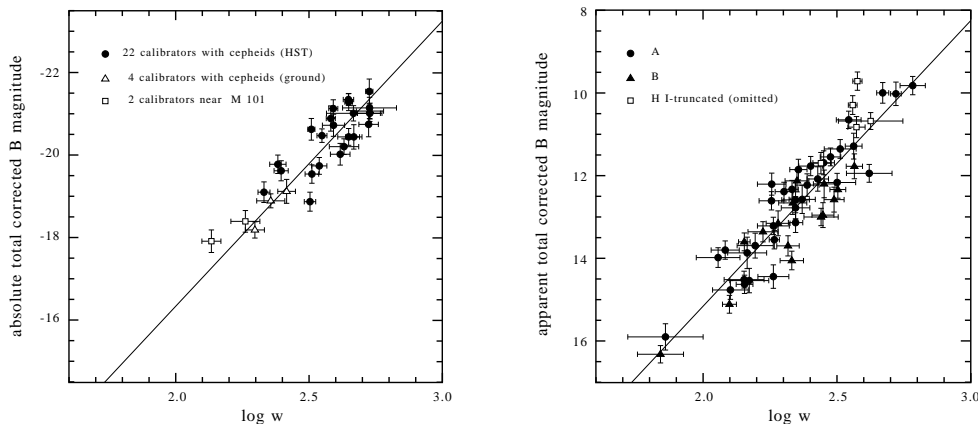


FIGURE 6. a) Tully - Fisher relation of 28 galaxies with independently known (Cepheid) distances. – b) Tully - Fisher relation for a complete sample of 49 Virgo cluster spirals.

TABLE 5. Additional distance determinations of the Virgo cluster.

Method	$(m - M)_{\text{Virgo}}$	original source
Globular Clusters	31.70 ± 0.30	Tammann & Sandage 1999
Novae	31.46 ± 0.40	Pritchett & van den Bergh 1987
$D_n - \sigma$	31.70 ± 0.15	Dressler 1987, Faber et al. 1998
mean:	31.66 ± 0.17	

to the bulges of S0-Sb galaxies. The mean of the two applications is given here. The zeropoint of the S0-Sb bulges is better determined than that of E/S0 galaxies, because the zeropoint of the latter depends on the assumption that the only two early-type galaxies of the Leo I group lie at the same distance as its spiral members. The results of the three methods are compiled in Table 5 and discussed in more detail by Tammann, Sandage, & Reindl (2000). The resulting mean distance modulus is in excellent agreement with the adopted value in Table 4 and is consistent with the assumption that early-type galaxies and spirals of the Virgo cluster are at the same distance.

Table 4 shows also the distance modulus of the Fornax cluster as derived from the three galaxies with Cepheids and three SNe Ia. The individual distances show much less scatter than in the case of the Virgo cluster; this is obviously a result of the smaller size and depth of the Fornax cluster.

For comparison with other distance indicators it is useful to have also the Cepheid and SNe Ia distance of the Leo I group. The relevant data are set out in Table 6. The adopted mean modulus is consistent with the GCLF distance (30.08 ± 0.29 ; Tammann & Sandage 1999) and the surface brightness fluctuation (SBF) distance (30.30 ± 0.06 ; Ferrarese et al. 2000).

Finally, it is noted that the distance of the Coma cluster relative to the Virgo cluster is well determined. The value $\Delta(m - M)_{\text{Coma-Virgo}} = 3.71 \pm 0.08$ (Tammann & Sandage 1999) from brightest cluster galaxies and the TF and $D_n - \sigma$ methods is quite uncontroversial. With the Virgo modulus in Table 4 one obtains $(m - M)_{\text{Coma}} = 35.31 \pm 0.22$ in

TABLE 6. The distance of the Leo I group.

Method (1)	Object (2)	$(m - M)^0$ (3)	Source (4)	Remarks (5)
Cepheids	NGC 3351	30.01 ± 0.15	Graham et al. 1997	
	NGC 3368	30.37 ± 0.16	Tanvir et al. 1995	
	NGC 3627	30.22 ± 0.12	Saha et al. 1999	
SNeIa	1998bu	30.32 ± 0.15	$m_{BVI}^{\text{corr}}(\text{max}) + \text{Table 2}$	in NGC 3368
mean:		30.23 ± 0.07		

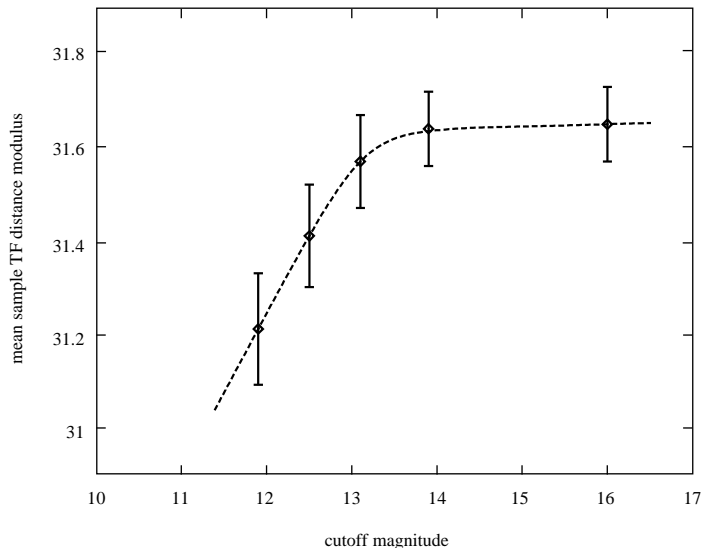


FIGURE 7. Illustration of the Teerikorpi cluster incompleteness bias. If the complete sample of 49 Virgo spirals is cut at levels brighter than $m_B \approx 13^m.5$ one derives too small TF distances. A cut at $m_B = 12^m.0$ introduces a distance modulus error of $0^m.4$ (20 percent in distance).

excellent agreement with the independently calibrated GCLF distance from *HST* (Baum et al. 1997; cf. Tammann & Sandage 1999).

3.4. The Teerikorpi cluster incompleteness bias

It is not the place here to discuss the Teerikorpi cluster incompleteness bias (Teerikorpi 1997 and references therein; Sandage, Tammann, & Federspiel 1995) in any detail, because it is well known that distance indicators with non-negligible internal scatter yield *too small distances* if applied to *incomplete* cluster samples.

For illustration the complete sample of 49 Virgo spirals as shown in Fig. 6b was cut at different apparent-magnitude limits, and each time the mean TF distance of the remaining sample was calculated. The mean distance of each sample increases monotonically with the depth of the cut. The result is shown in Fig. 7. The true, asymptotic distance is only reached if one samples $\sim 4^m.0$ into the cluster.

The bias effect explains why Sakai et al. (2000) have derived too high a value of H_0 by directly applying the TF calibration in Fig 6a to 15 clusters of Giovanelli et al. (1997).

TABLE 7. The absolute magnitude of 1st-ranked cluster galaxies.

Cluster	$m_{V_c}(1st)^1$	$(m - M)$	$M_V(1st)$
Virgo	8.21	31.60 ± 0.20	-23.39 ± 0.36
Fornax	8.83	31.65 ± 0.08	-22.82 ± 0.32
Coma	11.58	35.31 ± 0.22	-23.73 ± 0.39
mean:			-23.26 ± 0.20

¹ From Sandage & Hardy (1973). A scatter of 0^m32 is allowed for.

The shallow cluster samples are far from being complete and are bound to yield too small cluster distances. In fact the authors have derived $\langle H_0 \rangle = 86$ for the clusters whose distances rest on less than 10 members, while they have found $\langle H_0 \rangle = 70$ for the clusters with 10 to 28 members. *It is clear that more nearly complete samples would give still lower values of H_0 .*

3.5. The value of H_0 from clusters

The distances of the Virgo, Fornax, and Coma clusters in Section 3.3 yield the absolute magnitudes of three 1st-ranked cluster galaxies (Table 7). Inserting the mean value into equation (3.7) gives

$$H_0 = 51 \pm 7. \quad (3.9)$$

Combining alternatively the cluster distances relative to the Virgo cluster as given by equation (3.8) (cf. Fig. 5) with the Virgo cluster modulus of 31.60 ± 0.20 from Table 4 gives

$$H_0 = 56 \pm 6. \quad (3.10)$$

The result shows that once the Virgo cluster distance is fixed the value of H_0 has little leeway.

The relatively large error of the Virgo modulus is due to the important depth effect of the cluster. The four Cepheid and three SNe Ia distances do not suffice to sample the cluster in depth. The situation is aggravated by the fact that the Cepheid distances of three galaxies are biased because they were selected on the grounds of high resolution and hence must lie on the near side of the cluster. If one took unjustifiedly the mean distance of only these three Cepheids as the true cluster distance one would derive $H_0 = 72$.

Fortunately the SNe Ia, the most reliable distance indicators known, confirm the Virgo cluster distance estimated from Cepheids *and* the important depth of the cluster. Moreover, the now very solid Cepheid calibration of the TF relation finds its most powerful application in the complete sample of Virgo spirals and corroborates the conclusions from Cepheids and SNe Ia.

Kelson et al. (2000) have derived $H_0 = 75$ and 80 from the Hubble diagram based on $D_n - \sigma$ and FP data (Section 3.1.3). They have chosen certain distances of Leo I, Virgo, and Fornax for the calibration. Had they used the distances given in Table 4 and 6, they would have found $H_0 = 60(\pm 6)$ and $65(\pm 6)$, instead. This is a clear demonstration that the $D_n - \sigma$ /FP route to H_0 is in no way an independent method, but depends entirely on distances used as calibrators, and in particular on their distance of the Virgo cluster which we dispute. The power of H_0 from SNe Ia, the calibration of which only depends

on Cepheids, bypassing the still controversially discussed Virgo cluster distance, becomes here evident.

Lauer et al. (1998) have tried to calibrate the Hubble diagram of 1st-ranked cluster galaxies of Lauer & Postman (1992; Section 3.1.1) by means of the SBF method. For this purpose they have observed the SBF with *HST* of four 1st-ranked galaxies at $\sim 4300 \text{ km s}^{-1}$. On the unproven assumption that the fluctuation magnitude \overline{m}_I of these very particular objects is the same as in local E/S0 galaxies *and* spiral bulges, and adopting a local calibration magnitude \overline{M}_I , which in turn is controversial, they have derived distances of these four galaxies which they claim are in agreement with the turnover magnitudes m_I^T of the respective GCLFs. However, their calibrating turnover magnitude M_I^T rests entirely on *M 87*, which is known to have a peculiar bimodal GCLF, and on an adopted Virgo cluster modulus which is 0^m6 smaller than shown in Table 4 and 5. Thus, judging only from GCLFs their proposed value of $H_0 = 82$ should be reduced by a factor of 1.32 to give $H_0 = 62$. In any case their procedure appears like a complicated way – particularly in comparison to SNe Ia – to transport the Virgo cluster distance into the expansion field at $v \sim 10\,000 \text{ km s}^{-1}$.

4. H_0 from Field Galaxies

The most difficult and least satisfactory determination of H_0 comes from field galaxies. The difficulty comes from selection effects (Malmquist bias); the restricted impact comes from the fact that the method can hardly be carried beyond $\sim 5000 \text{ km s}^{-1}$ and hence does not necessarily reflect the large-scale value of H_0 .

The problem of selection effects is illustrated in Fig. 8b. 200 galaxies of constant space density and with $v < 5000 \text{ km s}^{-1}$ were randomly distributed in space by a Monte Carlo calculation. The “true” distances were expressed in velocities. It has further been assumed that the distance moduli of each galaxy had also been determined by the TF relation with an intrinsic scatter of $\sigma_{(m-M)} = \pm 0^m4$. The corresponding Hubble diagram in Fig. 8b gives the false impression as if the scatter would increase at larger distances; actually the increasing *number* of distant galaxies produces deviations by ± 2 or even ± 3 sigma. This makes the Hubble diagram “ugly” as compared to the one of SNe Ia in Fig. 8a (repeated here from Fig. 3 for comparison), but still the mean Hubble line through the points has the correct position *provided the sample is complete out to a given distance limit*. If, however, the sample is cut by an *apparent-magnitude limit* m_{lim} the Hubble line shifts upwards, resulting in too high a value of H_0 . With the present, realistically chosen parameters ($\langle M \rangle = -20.0$, $\sigma_M = 0^m4$, $H_0 = 60$, $m_{\text{lim}} = 13.0$) the overestimate of H_0 amounts to 14%. Samples which are not even complete to a given apparent-magnitude limit can give much larger systematic errors.

Another illustration of the Malmquist bias is given in the so-called Spaenhauer diagram (Fig. 9), where 500 galaxies were randomly distributed in space out to 42 Mpc using a Monte Carlo routine. The galaxies are assumed to scatter by $\sigma_M = 2^m0$ about a fixed mean luminosity of $M = -18.0$. If this distance-limited sample is cut by a limit in apparent magnitude a sample originates with very complex statistical properties. In particular the mean luminosity within any distance interval increases with distance. In the lower panel of Fig. 9 the increase amounts to $\Delta M = 2^m6$ which would overestimate H_0 by a factor of 3.3 if one were to force the local calibration of $M = -18.0$ on the most distant galaxies of the biased sample. For the sake of the argument the intrinsic dispersion of $\sigma_M = 2^m0$ was chosen here to be unrealistically large, but the effect is omnipresent in all apparent-magnitude-limited samples, *it always overestimates H_0* . Only if $\sigma_M \lesssim 0^m2$, as in the case of SNe Ia, the Malmquist bias becomes negligible. An additional crux of

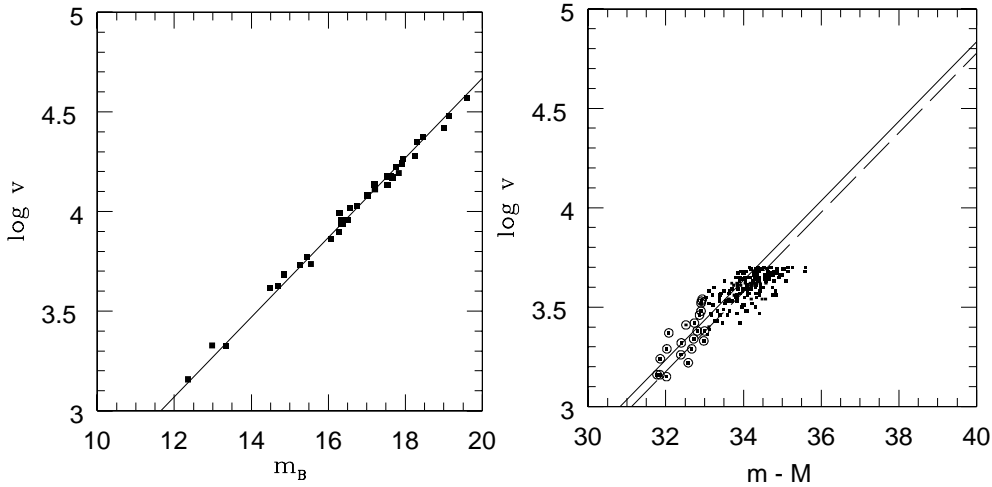


FIGURE 8. a) The Hubble diagram in B of SNe Ia (from Fig. 3; shown here only for comparison). b) The Hubble diagram of 200 galaxies with $v < 5000 \text{ km s}^{-1}$. Their velocities were assigned by a Monte Carlo calculation assuming constant space density. For each galaxy it was assumed that its TF distance has been determined within an intrinsic scatter of $0^m 4$. For the calibration of the abscissa it was assumed that all galaxies have a true absolute magnitude of $M = -20.0$ and that $H_0 = 60$. The dashed line is the best fit of the Hubble line for all points. The galaxies with *apparent* magnitude $m < 13.0$ are shown as large symbols. They define a Hubble line (full line) which is $0^m 29$ brighter, corresponding to a too high value of H_0 .

the bias is that the observable scatter within any distance interval *is always smaller than the true intrinsic scatter*. This has misled several authors to assume that σ_M is small and hence to underestimate the importance of bias.

There is an additional statistical difficulty as to the derivation of H_0 from field galaxies. Frequently H_0 is determined from the arithmetic mean of many values of H_i found from individual field galaxies. The underlying assumption is that the values H_i have a Gaussian distribution which is generally not correct. If the distance errors are symmetric in the moduli ($m - M$), they are not in linear distance r and consequently cause a skewness of H_i towards high values. An actual example is provided by the bias-corrected TF distances of 155 field galaxies with $v < 1000 \text{ km s}^{-1}$. A simple arithmetic mean of their corresponding H_i values, which have a non-Gaussian distribution, would give $\langle H_i \rangle = 64 \pm 2$, while the median value is 60.0 ± 3 . Yet a more nearly correct solution is given by averaging the values $\log H_i$, which have a perfect Gaussian distribution. This then gives the best estimate of $H_0 = 58 \pm 2$ (Federspiel 1999).

Unfortunately, the hope that the inverse TF relation (line width versus magnitude) was bias-free (Sandage, Tammann, & Yahil 1979; Schechter 1980) has been shattered (Teerikorpi et al. 1999).

Strategies have been developed to correct for Malmquist bias, particularly in the case of the (direct) TF relation, by e.g., Sandage (1988b, 1995) and Federspiel, Sandage, & Tammann (1994) and similarly by Teerikorpi (1994, 1997), Bottinelli et al. (1986, 1995), and Theureau (2000).

A selection of H_0 values, which have been derived from magnitude-limited, yet bias-corrected samples of field galaxies have been compiled in Table 8. The conclusion is

$$H_0 = 55 \pm 5 \quad (4.11)$$

from field galaxies, which is valid within various distance ranges up to $\sim 5000 \text{ km s}^{-1}$. It

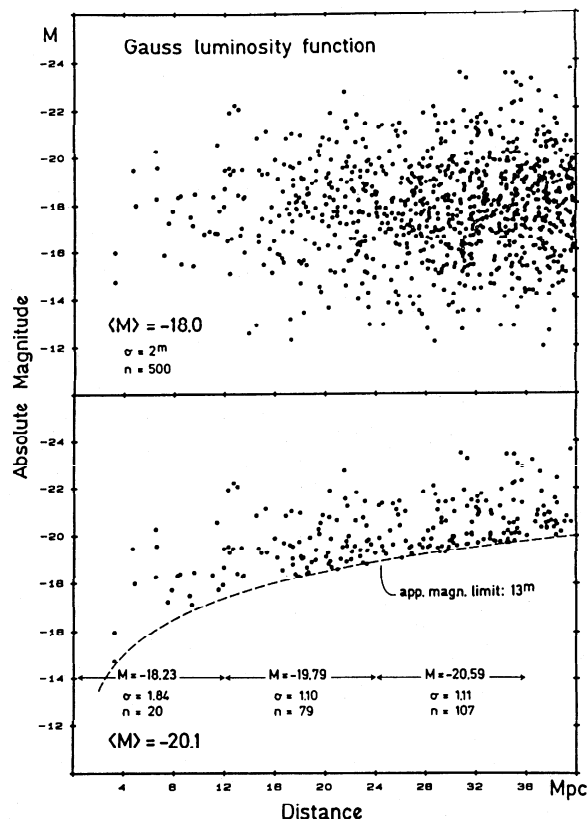


FIGURE 9. *Upper panel:* Monte Carlo calculation of the distance and absolute magnitude of 500 galaxies with constant space density and $r < 42$ Mpc. Their mean absolute magnitude is $\langle M \rangle = -18.0$ with an intrinsic scatter of $\sigma_M = 2^m$. *Lower panel:* The same distribution cut by an apparent-magnitude limit $m < 13.0$. Note that the mean luminosity of the magnitude-limited sample increases with distance.

should be noted that the different methods use spirals only – except the $D_n - \sigma$ entry – and their calibration rests only on Cepheids, independent of any adopted distance of the Virgo cluster.

Tonry et al. (2000) have derived $H_0 = 77 \pm 4$ from the SBF of 300 field galaxies with $v \lesssim 4000$ km s $^{-1}$ and on the basis of a very specific flow model. However, the usefulness of the SBF method has never been tested beyond doubt; a Hubble diagram of field galaxies and a corresponding determination of the intrinsic scatter of the method and hence of the importance of the Malmquist bias are still missing. The authors state correctly “The level of this Malmquist-like bias in our sample is difficult to quantify . . . and we may also be subject to possible biases and selection effects which depend on distance.” Moreover, in discussing Table 3 it was noted that the small relative SBF distance Virgo-Leo and the large value Fornax-Virgo are in serious contradiction to the evidence of Cepheids and SNe Ia. It is well possible that the SBF method is still affected by hidden second-parameter effects.

TABLE 8. Values of H_0 from field galaxies corrected for Malmquist bias.

Method (1)	H_0 (2)	Range [km s ⁻¹] (3)	Source (4)
Luminosity classes	56 ± 5	4000	Sandage 1996a
Morphol. twins of M 31, M 101	50 ± 5	5000	Sandage 1996b
TF (using mag. + diam.)	55 ± 5	5000	Theureau et al. 1997
Galaxy diam.	50 – 55	5000	Goodwin et al. 1997
TF	53 ± 5	500	Federspiel 1999
	58 ± 2	1000	”
Luminosity classes	55 ± 3	4000	Sandage 1999
$D_n - \sigma$	52 ± 8	4000	Federspiel 1999
TF (using mag. + diam.)	55 ± 5	8000	Theureau 2000
Morphol. twins of M 31, M 81	60 ± 10	5000	Paturel et al. 1998
Inverse TF	53 ± 6	8000	Ekhholm et al. 1999

5. Conclusions

The exceptionally tight Hubble diagram of blue SNe Ia out to $\sim 30\,000$ km s⁻¹ combined with their mean absolute magnitude, which is determined from eight galaxies whose Cepheid distances have been determined with *HST*, offers the ideal instrument for the calibration of the large-scale value of H_0 . The result is – after allowance is made for the relatively weak dependence of SNe Ia luminosities on decline rate Δm_{15} and color and for some small systematic effects – $H_0 = 58.5 \pm 6.3$.

The quoted external error is mainly determined by the calibrating Cepheid distances. Although Cepheids are generally considered to be the most reliable distance indicators, certain questions remain as to their zeropoint calibration through LMC and the effect of metallicity variations.

Phillips et al. (1999) and Suntzeff et al. (1999) have adopted a steeper relation between the SNe Ia luminosity and the decline rate Δm_{15} , which is not supported by the present larger sample. If their steep slope is taken at face value H_0 would be increased by 5 percent. Gibson et al. (2000) have increased the Cepheid distances of Saha et al. and Tanvir et al. in Table 2 by 0^m11 on average on the basis of additional Cepheids of lower weight. This would increase H_0 by another 5 percent. If one chooses to cumulate the two effects one could defend a value of $H_0 = 64$ (cf. Freedman 2000).

The calibration of H_0 through the Hubble diagram of clusters and through field galaxies in Section 3 and 4 has given values around $H_0 = 55$, i.e. somewhat smaller, if anything, than the value from SNe Ia. Since the latter offer the most direct way to H_0 , they are given the highest weight. A value of

$$H_0 = 58 \pm 6. \quad (5.12)$$

is therefore adopted as the best estimate available at present.

The two most frequent errors in the extragalactic distance scale, which can lead to values of $H_0 > 65$, are too small a Virgo cluster distance and Malmquist bias.

The distance of the Virgo cluster is still sometimes equated to the mean Cepheid distance of three Virgo spirals which are visibly on the near side of the cluster due to their high resolution into stars, – in fact they had been preselected on grounds of their high resolution to facilitate work with *HST*. Thus, – even if the larger cluster distance of $(m - M)_{\text{Virgo}} = 31.60 \pm 0.20$ (cf. Table 4 and 5) was not required by a fourth Cepheid

distance of a bona fide cluster member (NGC 4639) and in addition by the three SNe Ia and the TF relation, – the three Cepheid distances of highly resolved galaxies could set only a lower limit on the cluster distance, i.e. $(m - M)_{\text{Virgo}} > 31.05$.

The distance of the Virgo cluster has entered with high or even full weight into the zeropoint calibration of the $D_n - \sigma$, FP, and SBF methods and occasionally even of the turnover magnitude of the GCLF. (The significance of the GCLF, although not yet proven beyond doubt, is just that the calibration rests on the Cepheid distance of M 31 and on the RR Lyr distances of Galactic globular clusters [cf. Tammann & Sandage 1999]). If one inserts in these cases too low a Virgo cluster distance, one obtains incorrect values of $H_0 \approx 70$, or even more, by necessity.

Locally calibrated distance indicators with non-negligible scatter can exclusively be applied to distance-limited samples (or volume-limited samples in case of clusters), but only apparent-magnitude-limited samples are available, which frequently are not even complete to any specific magnitude limit. The statistical differences between a distance- and magnitude-limited sample are known for almost eighty years (Malmquist 1920, 1922), but this insight is violated again and again, always leading to too high values of H_0 . Malmquist's message is that control of the objects missing out to a fixed distance from a magnitude-limited catalog is equally important as the catalog entries themselves.

The future will see high-weight determinations of H_0 from the Sunyaev-Zeldovich effect, from gravitationally lensed quasars, and from the CMB fluctuations. At present these methods yield values of $50 \lesssim H_0 \lesssim 70$, which is not yet competitive with the solution of SNe Ia. In the case of the CMB fluctuations one can solve for H_0 only in combination with other (poorly known) cosmological parameters. Therefore an *independent*, high-accuracy determination of H_0 , to be used as a prior, is as important as ever.

Acknowledgement. The authors thank Bernd Reindl, Daniel Cerrito, and Hans Schwengeler for their most valuable help in preparing the manuscript. G.A.T. acknowledges financial support of the Swiss National Science Foundation.

REFERENCES

- ALIBERT, ET AL. 1999, Period-luminosity-color-radius relationships of Cepheids as a function of metallicity: evolutionary effects, *A&A* **344**, 551.
- BAUM, W.A., HAMMERGREN, M., THOMSEN, B., GROTH, E.J., FABER, S.M., GRILLMAIR, C.J., & AJHAR, E.A. 1997, Distance to the Coma Cluster and a Value for H_0 Inferred from Globular Clusters in IC 4051, *AJ* **113**, 1483.
- BINGGELI, B., POPESCU, C.C., & TAMMANN, G.A. 1993, The kinematics of the Virgo cluster revisited, *A&AS* **98**, 275.
- BINGGELI, B., SANDAGE, A., & TAMMANN, G.A. 1985, Studies of the Virgo Cluster. II – A catalog of 2096 galaxies in the Virgo Cluster area, *AJ* **90**, 1681.
- BOTTINELLI, L., GOUGUENHEIM, L., PATUREL, G., & TEERIKORPI, P. 1986, The Malmquist bias and the value of H_0 from the Tully-Fisher relation, *A&A* **156**, 157.
- BOTTINELLI, L., GOUGUENHEIM, L., PATUREL, G., & TEERIKORPI, P. 1991, A systematic effect in the use of planetary nebulae as standard candles, *A&A* **252**, 550.
- BOTTINELLI, L., GOUGUENHEIM, L., PATUREL, G., & TEERIKORPI, P. 1995, Extragalactic database. VI. Inclination corrections for spiral galaxies and disk opaqueness in the B-band, *A&A* **296**, 64.
- BRANCH, D. 1998, Type Ia Supernovae and the Hubble Constant, *ARA&A* **36**, 17.
- CARROLL, S.M., PRESS, W.H., & TURNER, E.L. 1992, The cosmological constant, *ARA&A* **30**, 499.

- CAPACCIOLI, M., DELLA VALLE, M., & D'ONOFRIO, M. 1989, Properties of the nova population in M31, *AJ* **97**, 1622.
- DALE, D.A., GIOVANELLI, R., HAYNES, M.P., CAMUSANO, L.E., & HARDY, E. 1999, Seeking the Local Convergence Depth. V. Tully-Fisher Peculiar Velocities for 52 Abell Clusters, *AJ* **118**, 1489.
- DRESSLER, A. 1987, The $D_n - \sigma$ relation for bulges of disk galaxies - A new, independent measure of the Hubble constant, *ApJ* **317**, 1.
- EKHOLM, T., TEERIKORPI, P., THEUREAU, G., HANSKI, M., PATUREL, G., BOTTINELLI, L., & GOUGUENHEIM, L. 1999, Kinematics of the local Universe. X. H_0 from the inverse B-band Tully-Fisher relation using diameter and magnitude limited samples, *A&A* **347**, 99.
- FABER, S.M., ET AL. 1989, Spectroscopy and photometry of elliptical galaxies. VI - Sample selection and data summary, *ApJS* **69**, 763.
- FEAST, M.W. 1999, Cepheids as Distance Indicators, *PASP* **111**, 775.
- FEDERSPIEL, M. 1999, Kinematic Parameters of Galaxies as Distance Indicators, Ph.D. thesis, Univ. of Basel.
- FEDERSPIEL, M., SANDAGE, A., & TAMMANN, G.A. 1994, Bias properties of extragalactic distance indicators. III: Analysis of Tully-Fisher distances for the Mathewson-Ford-Buchhorn sample of 1355 galaxies, *ApJ* **430**, 29.
- FEDERSPIEL, M., TAMMANN, G.A., & SANDAGE, A. 1998, The Virgo Cluster Distance from 21 Centimeter Line Widths, *ApJ* **495**, 115.
- FERRARESE, L., ET AL. 1996, The Extragalactic Distance Scale Key Project. IV. The Discovery of Cepheids and a New Distance to M100 Using the Hubble Space Telescope, *ApJ* **464**, 568.
- FERRARESE, L., ET AL. 2000, The Hubble Space Telescope Key Project on the Extragalactic Distance Scale. XXVI. The Calibration of Population II Secondary Distance Indicators and the Value of the Hubble Constant, *ApJ* **529**, 745.
- FREEDMAN, W.L. 2000, this volume.
- GARNAVICH, P.M., RIESS, A.G., KIRSHNER, R.P., CHALLIS, P. & WAGNER, R.M. 1996, The Spectroscopically Peculiar Supernovae 1995ac and 1995bd: 91T and Beyond, *A&AS* **189**, 4509.
- GIBSON, B.K., ET AL. 2000, The *HST* Key Project on the Extragalactic Distance Scale. XXV. A Recalibration of Cepheid Distances to Type Ia Supernovae and the Value of the Hubble Constant, *ApJ* **529**, 723.
- GILMOZZI, R. & PANAGIA, N. 1999, Space Telescope Science Institute Preprint Series, No. 1319.
- GIOVANELLI, R. 1997, private communication.
- GIOVANELLI, R., ET AL. 1997, The I Band Tully-Fisher Relation for Cluster Galaxies: Data Presentation, *AJ* **113**, 22.
- GOODWIN, S.P., GRIBBIN, J., & HENDRY, M.A. 1997, A New Determination of the Hubble Parameter Using Galaxy Linear Diameters, *AJ* **114**, 2212.
- GRAHAM, J.A., ET AL. 1999, The Hubble Space Telescope Key Project on the Extragalactic Distance Scale. XX. The Discovery of Cepheids in the Virgo Cluster Galaxy NGC 4548, *ApJ* **516**, 626.
- GRATTON, R. 2000, RR Lyrae stars and Cepheids from HIPPARCOS, in *XIXth. Texas Symposium on Relativistic Astrophysics and Cosmology*, eds. E. Aubourg, et al., Mini-symposium 13/03.
- HÖFLICH, P.H. & KHOKHLOV, A. 1996, Explosion Models for Type Ia Supernovae: A Comparison with Observed Light Curves, Distances, H_0 , and q_0 , *ApJ* **457**, 500.
- JERJEN, H., & TAMMANN, G.A. 1993, The Local Group Motion Towards Virgo and the Microwave Background, *A&A* **276**, 1.
- JHA, S., ET AL. 1999, The Type Ia Supernova 1998BU in M96 and the Hubble Constant, *ApJS* **125**, 73.
- KELSON, D.D., ET AL. 2000, The Hubble Space Telescope Key Project on the Extragalactic

- Distance Scale. XXVII. A Derivation of the Hubble Constant Using the Fundamental Plane and $D_n - \sigma$ Relations in Leo I, Virgo, and Fornax, *ApJ* **529**, 768.
- KENNICUTT, R.C., ET AL. 1998, The Hubble Space Telescope Key Project on the Extragalactic Distance Scale. XIII. The Metallicity Dependence of the Cepheid Distance Scale, *ApJ* **498**, 181.
- KRAAN-KORTEWEG, R.C. 1986, A catalog of 2810 nearby galaxies – The effect of the Virgocentric flow model on their observed velocities, *A&AS* **66**, 255.
- LANOIX, P. 1998, HIPPARCOS calibration of the peak brightness of four SNe Ia and the value of H_0 , *A&A* **331**, 421.
- LANOIX, P., PATUREL, G., & GARNIER, R. 1999, Bias in the Cepheid Period-Luminosity Relation, *ApJ* **517**, 188.
- LAUER, T.R., & POSTMAN, M. 1992, The Hubble flow from brightest cluster galaxies, *ApJ* **400**, L47.
- LAUER, T.R., ET AL. 1998, The Far-Field Hubble Constant, *ApJ* **499**, 577.
- LIVIO, M. 1997, Novae as distance indicators, in *The Extragalactic Distance Scale*, eds. M. Livio, M. Donahue, & N. Panagia, (Cambridge: Cambridge Univ. Press), p. 186.
- MADORE, B., & FREEDMAN, W.L. 1998, Hipparcos Parallaxes and the Cepheid Distance Scale, *ApJ* **492**, 110.
- MACRI, L.M., ET AL. 1999, The Extragalactic Distance Scale Key Project. XVIII. The Discovery of Cepheids and a New Distance to NGC 4535 Using the Hubble Space Telescope, *ApJ* **521**, 155.
- MALMQUIST, K.G. 1920, A study of the stars of spectral type A, *Lund Medd. Ser. II* **22**, 1.
- MALMQUIST, K.G. 1922, On some relations in stellar statistics, *Lund Medd. Ser. I* **100**, 1.
- MAZUMDAR, A. & NARASIMHA, D. 2000, Calibration of Cepheid characteristics relevant to the distance scale, preprint.
- MÉNDEZ, R.H., KUDRITZKI, R.P., CIARDULLO, R., & JACOBY, G.H. 1993, The bright end of the planetary nebula luminosity function, *A&A* **275**, 534.
- MOULD, J.R., ET AL. 2000, The Hubble Space Telescope Key Project on the Extragalactic Distance Scale. XXI. The Cepheid Distance to NGC 1425, *ApJ* **528**, 655.
- PARODI, B.R., SAHA, A., SANDAGE, A., & TAMMANN, G.A. 2000, Supernova Type Ia Luminosities and Their Dependence on Second Parameters, *ApJ*, in press.
- PATUREL, ET AL. 1998, Hubble constant from sosie galaxies and HIPPARCOS geometrical calibration, *A&A* **339**, 671.
- PERLMUTTER, S. 1998, Measurements of Ω and Λ from Supernovae, in *Supernovae and Cosmology*, eds. L. Labhardt, B. Binggeli, & R. Buser, (Basel: Astronomisches Institut der Universität Basel), p. 75.
- PERLMUTTER, S., ET AL. 1999, Measurements of Omega and Lambda from 42 High-Redshift Supernovae, *ApJ* **517**, 565.
- PHILLIPS, M.M. 1993, The absolute magnitudes of Type Ia supernovae, *ApJ* **413**, 105.
- PHILLIPS, M. M., WELLS, L.A., SUNTZEFF, N.B., HAMUY, M., LEIBUNDGUT, B., KIRSHNER, R.P., & FOLTZ, C.B. 1992, SN 1991T - Further evidence of the heterogeneous nature of type Ia supernovae, *AJ* **103**, 1632.
- PHILLIPS, M.M., LIRA, P., SUNTZEFF, N.B., SCHOMMER R.A., HAMUY, M., & MAZA, J. 1999, The Reddening-Free Decline Rate Versus Luminosity Relationship for Type Ia Supernovae, *AJ* **118**, 1766.
- PROSSER, C.F., ET AL. 1999, The Hubble Space Telescope Key Project on the Extragalactic Distance Scale. XXII. The Discovery of Cepheids in NGC 1326A, *ApJ* **525**, 80.
- PRITCHET, C.J., & VAN DEN BERGH, S. 1987, Observations of novae in the Virgo cluster, *ApJ* **318**, 507.
- RICHTLER, T., & DRENKHAN, G. 1999, The Hubble Constant from Type Ia Supernovae in Early-Type Galaxies, in *Cosmology and Astrophysics: A collection of critical thoughts*, eds. W. Kundt & C. van de Bruck, Lecture Notes in Physics, (Berlin: Springer), astro-

ph/99 09 117.

- RIESS, A.G., ET AL. 1998, Observational Evidence from Supernovae for an Accelerating Universe and a Cosmological Constant, *AJ* **116**, 1009.
- SAHA, A., LABHARDT, L., SCHWENGELER, H., MACCHETTO, F.D., PANAGIA, N., SANDAGE, A., & TAMMANN, G.A. 1994, Discovery of Cepheids in IC 4182: Absolute peak brightness of SN Ia 1937C and the value of H_0 , *ApJ* **425**, 14.
- SAHA, A., SANDAGE, A., LABHARDT, L., SCHWENGELER, H., TAMMANN, G.A., PANAGIA, N., & MACCHETTO, F.D. 1995, Discovery of Cepheids in NGC 5253: Absolute peak brightness of SN Ia 1895B and SN Ia 1972E and the value of H_0 , *ApJ* **438**, 8.
- SAHA, A., SANDAGE, A., LABHARDT, L., TAMMANN, G.A., MACCHETTO, F.D., & PANAGIA, N. 1996a, Cepheid Calibration of the Peak Brightness of SNe Ia. V. SN 1981B in NGC 4536, *ApJ* **466**, 55.
- SAHA, A., SANDAGE, A., LABHARDT, L., TAMMANN, G.A., MACCHETTO, F.D., & PANAGIA, N. 1996b, Cepheid Calibration of the Peak Brightness of SNe Ia. V. SN 1981B in NGC 4536, *ApJS* **107**, 693.
- SAHA, A., SANDAGE, A., LABHARDT, L., TAMMANN, G.A., MACCHETTO, F.D., & PANAGIA, N. 1997, Cepheid Calibration of the Peak Brightness of Type Ia Supernovae. VIII. SN 1990N in NGC 4639, *ApJ* **486**, 1.
- SAHA, A., SANDAGE, A., TAMMANN, G.A., LABHARDT, L., MACCHETTO, F.D., & PANAGIA, N. 1999, Cepheid Calibration of the Peak Brightness of Type Ia Supernovae. IX. SN 1989B in NGC 3627, *ApJ* **522**, 802.
- SAHA, A., SANDAGE, A., THIM, F., LABHARDT, L., TAMMANN, G.A., MACCHETTO, F.D., & PANAGIA, N. 2000a, Cepheid Calibration of the Peak Brightness of SNe Ia. X. SN 1991T in NGC 4527, *ApJ*, in press.
- SAHA, A., LABHARDT, L., & PROSSER, C. 2000b, On Deriving Distances from Cepheids Using the Hubble Space Telescope, *PASP* **112**, 163.
- SAKAI, S., ZWITSKY, D., & KENNICUTT, R.C. 2000, The Tip of the Red Giant Branch Distance to the Large Magellanic Cloud, *AJ* **119**, 1197.
- SAKAI, S., ET AL. 2000, The Hubble Space Telescope Key Project on the Extragalactic Distance Scale. XXIV. The Calibration of Tully-Fisher Relations and the Value of the Hubble Constant, *ApJ* **529**, 698.
- SANDAGE, A. 1961, The Ability of the 200-inch Telescope to Discriminate Between Selected World Models, *ApJ* **133**, 355.
- SANDAGE, A. 1962, The Change of Redshift and Apparent Luminosity of Galaxies due to the Deceleration of Selected Expanding Universes, *ApJ* **136**, 319.
- SANDAGE, A. 1988, Cepheids as distance indicators when used near their detection limit, *PASP* **100**, 935.
- SANDAGE, A. 1988, A case for $H_0 = 42$ and $\Omega_0 = 1$ using luminous spiral galaxies and the cosmological time scale test, *ApJ* **331**, 583.
- SANDAGE, A. 1995, Practical Cosmology: Inverting the Past, in *The Deep Universe*, eds. B. Binggeli & R. Buser, (Springer: Berlin), p. 210.
- SANDAGE, A. 1996a, Bias Properties of Extragalactic Distance Indicators. V. H_0 From Luminosity Functions of Different Spiral Types and Luminosity Classes Corrected for Bias, *AJ* **111**, 1.
- SANDAGE, A. 1996b, Bias Properties of Extragalactic Distance Indicators. VI. Luminosity Functions of M 31 and M 101 Look-alikes Listed in the RSA2: H_0 Therefrom, *AJ* **111**, 18.
- SANDAGE, A. 1999, Bias Properties of Extragalactic Distance Indicators. VIII. H_0 from Distance-limited Luminosity Class and Morphological Type-Specific Luminosity Functions for Sb, Sbc, and Sc Galaxies Calibrated Using Cepheids, *ApJ* **527**, 479.
- SANDAGE, A., & BEDKE, J. 1988, *Atlas of Galaxies useful to measure the Cosmological Distance Scale*, (NASA: Washington).
- SANDAGE, A., BELL, R.A., & TRIPICCO, M.J. 1999, On the Sensitivity of the Cepheid Period-Luminosity Relation to Variations of Metallicity, *ApJ* **522**, 250 .

- SANDAGE, A., & HARDY, E. 1973, The Redshift-Distance Relation. VII. Absolute Magnitudes of the First Three Ranked Cluster Galaxies as Functions of Cluster Richness and Bautz-Morgan Cluster Type: the Effect of q_0 , *ApJ* **183**, 743.
- SANDAGE, A., TAMMANN, G.A., & FEDERSPIEL, M. 1995, Bias Properties of Extragalactic Distance Indicators. IV. Demonstration of the Population Incompleteness Bias Inherent in the Tully-Fisher Method Applied to Clusters, *ApJ* **452**, 1.
- SANDAGE, A., TAMMANN, G.A., & YAHIL, A. 1979, The velocity field of bright nearby galaxies. I - The variation of mean absolute magnitude with redshift for galaxies in a magnitude-limited sample, *ApJ* **232**, 352.
- SCHECHTER, P.L. 1980, Mass-to-light ratios for elliptical galaxies, *AJ* **85**, 801.
- SCHLEGEL, D., FINKBEINER, D., & DAVIS, M. 1998, Maps of Dust Infrared Emission for Use in Estimation of Reddening and Cosmic Microwave Background Radiation Foregrounds, *ApJ* **500**, 525.
- SCHMIDT, B., ET AL. 1998, The High-Z Supernova Search: Measuring Cosmic Deceleration and Global Curvature of the Universe Using Type Ia Supernovae, *ApJ* **507**, 46.
- SCHRÖDER, A. 1995, Ph.D. thesis, Univ. of Basel.
- SILBERMANN, N.A., ET AL. 1999, The Hubble Space Telescope Key Project on the Extragalactic Distance Scale. XIV. The Cepheids in NGC 1365, *ApJ* **515**, 1.
- SOFFNER, T., MÉNDEZ, R., JACOBY, G., CIARDULLO, R., ROTH, M., & KUDRITZKI, R. 1996, Planetary nebulae and HII regions in NGC 300, *A&A* **306**, 9.
- STANEK, K.Z., & UDALSKI, A. 1999, The Optical Gravitational Lensing Experiment. Investigating the Influence of Blending on the Cepheid Distance Scale with Cepheids in the Large Magellanic Cloud, preprint, astro-ph/99 09 346 .
- SUNTZEFF, N.B., ET AL. 1999, Optical Light Curve of the Type Ia Supernova 1998BU in M 96 and the Supernova Calibration of the Hubble Constant, *AJ* **117**, 1175.
- TAMMANN, G.A. 1982, Supernova statistics and related problems, in *Supernovae: A Survey of Current Research*, eds. M.J. Rees & R.J. Stoneham, (Dordrecht: Reidel), p. 371.
- TAMMANN, G.A. 1993, Why are Planetary Nebulae Poor Distance Indicators? in *Planetary Nebulae*, eds. R. Weinberger & A. Acker, IAU Symp. 155, (Dordrecht: Kluwer), p. 515.
- TAMMANN, G.A., & FEDERSPIEL, M. 1997, Focusing in on H_0 , in *The Extragalactic Distance Scale*, eds. M. Livio, M. Donahue, & N. Panagia, (Cambridge: Cambridge Univ. Press), p. 137.
- TAMMANN, G.A., & SANDAGE, A. 1999, The Luminosity Function of Globular Clusters as an Extragalactic Distance Indicator, in *Harmonizing Cosmic Distance Scales in a Post-Hipparcos Era*, eds. D. Egret & A. Heck, p. 204.
- TAMMANN, G.A., SANDAGE, A., & REINDL, B. 2000, The Distance of the Virgo Cluster, in *XIXth. Texas Symposium on Relativistic Astrophysics and Cosmology*, eds. E. Aubourg, et al., Mini-Symposium 13/11.
- TANVIR, N.R., SHANKS, T., FERGUSON, H.C., & ROBINSON, D.R.T. 1995, Determination of the Hubble constant from observations of Cepheid variables in the galaxy M 96, *Nature* **377**, 27.
- TEERIKORPI, P. 1984, Malmquist bias in a relation of the form $M = aP + b$, *A&A* **141**, 407.
- TEERIKORPI, P. 1997, Observational Selection Bias Affecting the Determination of the Extragalactic Distance Scale, *ARA&A* **35**, 101.
- TEERIKORPI, P., EKHOLM, T., HANSKI, M.O., & THEUREAU, G. 1999, Theoretical aspects of the inverse Tully-Fisher relation as a distance indicator: incompleteness in $\log V_{\text{Max}}$, the relevant slope, and the calibrator sample bias, *A&A* **343**, 713.
- THEUREAU, G. 2000, Tully-Fisher distances of field galaxies and the value of H_0 , in *XIXth. Texas Symposium on Relativistic Astrophysics and Cosmology*, eds. E. Aubourg, et al., Mini-Symposium 13/12.
- THEUREAU, G., HANSKI, M., EKHOLM, T., BOTTINELLI, L., GOUGUENHEIM, L., PATUREL, G., & TEERIKORPI, P. 1997, Kinematics of the Local Universe. V. The value of H_0 from the Tully-Fisher B and $\log D_{25}$ relations for field galaxies, *A&A* **322**, 730.

- TONRY, J.L., BLAKESLEE, J.P., AJHAR, E.A., & DRESSLER, A. 2000, The Surface Brightness Fluctuation Survey of Galaxy Distances. II. Local and Large-Scale Flows, *ApJ* **530**, 625.
- TRIPP, R. 1998, A two-parameter luminosity correction for Type Ia supernovae, *A&A* **331**, 815.
- TRIPP, R., & BRANCH, D. 1999, Determination of the Hubble Constant Using a Two-Parameter Luminosity Correction for Type Ia Supernovae, *ApJ* **525**, 209.
- TURNER, A., ET AL. 1998, The Hubble Space Telescope Key Project on the Extragalactic Distance Scale. XI. The Cepheids in NGC 4414, *ApJ* **505**, 207.
- WALKER, A.R. 1999, The Distances of the Magellanic Clouds, in *Post-Hipparcos cosmic candles*, eds. A. Heck and F. Caputo, (Dordrecht: Kluwer Academic Publishers), p. 125.
- WEEDMAN, D. 1976, The Hubble diagram for nuclear magnitudes of cluster galaxies, *ApJ* **203**, 6.